Engineering Analysis with Boundary Elements 97 (2018) 67–81

Contents lists available at ScienceDirect

Engineering Analysis with Boundary Elements

journal homepage: www.elsevier.com/locate/enganabound

Practical boundary element method for piled rafts

Osama E. Shehata[a], Ahmed Fady Farid[a,*], Youssef F. Rashed[a,b]

[a] Department of Structural Engineering, Cairo University, Giza, Egypt
[b] Supreme Council of Universities in Egypt, Giza, Egypt

ARTICLE INFO

Keywords:
Boundary element method
Stiffness matrix
Interaction factors
Pile–pile interaction
Rafts
Piled rafts

ABSTRACT

In this paper, a practical boundary element method (BEM) is developed to analyze piled rafts. The raft is modeled using the direct boundary element formulation for thick plates; which is suitable for such type of problems. An innovative methodology to add stiffness matrices to the plate integral equations is developed. Hence, pile–soil–raft interactions are added as a special case of the developed methodology. In order to avoid generating huge systems of coupled equations, an effective condensation technique of piles and soil degrees of freedom (DOFs) at pile–soil–raft interface is employed. Several numerical examples are presented and results are compared to previously published results. Then, a practical application is solved to demonstrate the strength and versatility of the proposed formulation.

1. Introduction

Piled rafts are an important type of foundations for tall buildings. This type is suitable to overcome both bearing capacity and settlement problems. A typical review of such importance is presented in Refs. [1–4]. Therefore, accurate modeling of piled raft components: plate, soil, and piles is essential in foundation structural analysis.

Plates rested on soil could be represented as plates over Winkler springs or over elastic half space (EHS). The Winkler model represents the soil as individual springs as in the work of Coduto [5]. Analysis of plates over elastic foundations (Winkler or EHS) were considered using the finite element method as in the work of Cheung and Zienkiewicz [6], Svec and McNeice [7], Svec and Gladwel [8] for thin plates, and Rajapaks and Selvadurai [9] for thick plates. Examples of using the boundary element method for such a problem are the work of Katsikadelis and Armenakas [10], Syngellakis and Bai [11], Paiva and Butterfield [12] for thin plates, and Rashed and co-workers [13–16] for thick plates.

Alternatively, the soil could be modeled based on 3D finite elements or boundary elements. There are two methods to represent the soil using BEM. The first, as 3D boundary elements; which need enclosing boundaries as those of FEM. Such a technique has never been reported in the literature. The second way is to represent the 3D soil medium as elastic half space. It has be noted, that the second way was referred to, by almost all authors in the literature, as “using the boundary element method”, regardless of which numerical model of raft plate was used (either it was modeled using the FEM or the BEM).

Modeling piled rafts is more sophisticated than modeling plates on elastic foundations. Piles should be modeled as embedded in the soil continuum considering all interaction between piles, soil, and raft. The finite element method could be used to represent piled raft, in which three-dimensional solid elements [17] are used to model soil. It has to be noted that, such a model generates a large number of DOFs; therefore, it is inconvenient for practical applications. Alternatively, two-dimensional axisymmetric finite element [18] were used to model axisymmetric foundations, in which interaction effects were ignored. Such a model is also not practical, as it cannot model general practical foundations.

Paiva and co-workers [19,20] developed a BEM formulation for solving piled rafts, in which all the interactions were considered. In [19,20] the pile cap is divided into triangular thin finite elements, despite the conclusion of Small [21], which indicates that the use of thin plate theory may lead to inaccuracy in modeling thick foundations. All piles and soil in [19,20] were embedded in the problem integral equation; therefore, such formulation leads to a huge system of equations leading to difficulty in solving practical piled rafts.

Engineers and modelers, in design offices, tend to use approximate methods for piled raft analysis. They model such a foundation as plate resting on springs. The initial pile stiffness is computed based on empirical formulas according to design code equations [22] or obtained from pile–load test [23].

Few software packages that consider the effect of pile–pile interactions in piled raft analysis are available. ELPLA [24] represents the raft

* Corresponding author.
E-mail address: ahmedfadyfarid@eng1.cu.edu.eg (A.F. Farid).

https://doi.org/10.1016/j.enganabound.2018.09.009
Received 12 May 2018; Received in revised form 9 September 2018; Accepted 9 September 2018
0955-7997/© 2018 Elsevier Ltd. All rights reserved.

as thin plate via plate bending finite elements and considers interactions between piles/soil based on Mindlin's solution (The Elastic approach). LUSAS [25] uses thin/thick plate bending elements to simulate rafts. The soil is represented as 3D finite elements. Piles are modeled as beam elements inside the 3D soil continuum. PLAXIS [26], ABAQUS [27], and Midas [28] are alternative multi-purpose and general FEM based software packages. They could be used to analyze a piled raft system, in which the soil is modeled as 3D finite elements. Despite the spread of such approaches, they are not suitable for large practical applications.

It has to be noted that in all previously considered publications, all verification examples and solved problems (which in some publications referred to as "practical applications") are simple problems and cannot be regarded as practical applications.

In conclusion, in order to develop a practical numerical analysis for piled rafts, the following points should be considered:

(1) Suitable representation of raft as shear-deformable plate to account for the raft thickness.
(2) Suitable modeling of stress concentration due to presence of both pile reactions and applied column loads.
(3) Suitable numerical method to model large practical problems with large number of DOFs.
(4) Suitable implementation of all interaction effects.

This paper considers the boundary element method (BEM) for shear-deformable plates to model thick piled rafts. The use of BEM ensures the continuity of internal variables with no physical discretization as those in the FEM. This ensures the efficient and accurate modeling of singular internal field even when concentrated loads are presented, such as applied column loads or supporting pile reactions. Moreover, piles DOFs are condensed at the head of piles and added as additional stiffness to the integral equation of the plate. This developed technique reduces the number of DOFs considerably to allow solving large-scale problems as presented in Section 6. All interaction effects are considered. Pile–pile interactions is considered based on both the elastic approach [1,3] and the load transfer approach [2]. Pile–soil interactions is also considered based on Mindlin's solution [29]. Soil–soil interactions can be considered as well based on Mindlin's [29], Boussinesq's [30], and Steinbrenner's [31] solutions.

2. Boundary integral equations for plates in bending

In this section, the direct boundary element formulation for thick plates is reviewed. Consider a general thick plate of domain Ω and boundary Γ as shown in Fig. 1. The indicial notation is used, where the Greek indices vary from 1 to 2 and Roman indices vary from 1 to 3. The relevant integral equation could be written as follows:

$$C_{ij}(\xi)u_j(\xi)+\int_{\Gamma(x)} T_{ij}(\xi,x)u_j(x)\mathrm{d}\Gamma(x)=\int_{\Gamma(x)} U_{ij}(\xi,x)t_j(x)\mathrm{d}\Gamma(x)+L_1+L_2 \tag{1}$$

where $T_{ij}(\xi, x)$, $U_{ij}(\xi, x)$ are the two-point fundamental solution kernels for tractions and displacements respectively [15]. The two points ξ and x are the source and the field points respectively. $u_j(x)$ and $t_j(x)$ denote the boundary generalized displacements and tractions. $C_{ij}(\xi)$ is the free term. The integrals L_1, L_2 are the prescribed domain load integrals and could be defined as follows [32]:

$$L_1=\int_{\Gamma(x)}\left[V_{i,n}(\xi,x)-\frac{\nu}{(1-\nu)\lambda^2}U_{i\alpha}(\xi,x)n_\alpha(x)\right]q(x)\mathrm{d}\Gamma(x) \tag{2}$$

$$L_2=\sum_{N_{cell}}\int_{\Omega(L)}\left[U_{ik}(\xi,L)-\frac{\nu}{(1-\nu)\lambda^2}U_{i\alpha,\alpha}(\xi,L)\delta_{3k}\right]P_k(L)\mathrm{d}\Omega(L) \tag{3}$$

where $V_i(\xi, x)$ is a suitable particular solutions to account for uniform domain loading [15], other type of loading could be dealt with via cell loadings. The symbols ν and λ denote the plate Poisson's ratio and shear factor, respectively. $q(x)$ denotes the intensity of the uniform domain loading. N_{cell} denotes the number of loading cells that having domain denoted by Ω_L, P_k denotes the three prescribed loads (two moments and one force) for each loading cell. The field point L denotes the loading cell center.

After discretizing the boundary of the plate into N_{ele} quadratic elements, each node has three unknowns. Eq. (1) could be re-written in a matrix form as follows:

$$\underset{3N}{3N\boxed{[H]}}\times\underset{1}{3N\boxed{\{u\}}}=\underset{9\,N_{ele}}{3N\boxed{[G]}}\times\underset{1}{9\,N_{ele}\boxed{\{t\}}}+\underset{1}{3N\boxed{\{LV\}}} \tag{4}$$

where N is the number of nodes. $[H]$ and $[G]$ are the well-known influence matrices. The vector $\{LV\}$ contains prescribed domain loading and loading cells effects (L_1+L_2). After re-ordering the matrices in Eq. (4) to decouple the prescribed values from the unknown boundary values, Eq. (4) could be re-written as follows:

$$\underset{3N}{3N\boxed{[A]}}\times\underset{1}{3N\boxed{\begin{matrix}\{u\}\\ \text{or}\\ \{t\}\end{matrix}}}=\underset{1}{3N\boxed{\{LV\}-\{PBV\}}} \tag{5}$$

where the vector {PBV} contains prescribed boundary integral values and defined as follows:

$$\{\mathrm{PBV}\}=\begin{cases}-\int_\Gamma T^*_{ij}(\xi,x)\mathrm{d}\Gamma(x), & \text{if } u(x) \text{ is prescribed}\\ -\int_\Gamma U^*_{ij}(\xi,x)\mathrm{d}\Gamma(x), & \text{if } t(x) \text{ is prescribed}\end{cases} \tag{6}$$

3. The proposed integral equation for plates with additional stiffness

In the previous section, the direct boundary element formulation for a thick plate without any domain supporting substructures is reviewed. In this section, such a plate is reconsidered when additional domain supporting substructures (Ω_s) are present. If the plate in Fig. 1 is supported over (n) substructures (noting that each substructure is divided into a series of supporting cells), Eq. (1) could be re-written as follows:

$$C_{ij}(\xi)u_j(\xi)+\int_{\Gamma(x)}T_{ij}(\xi,x)u_j(x)\mathrm{d}\Gamma(x)=\int_{\Gamma(x)}U_{ij}(\xi,x)t_j(x)\mathrm{d}\Gamma(x)+L_1+L_2+\sum_{s=1}^{s=n}I_s \tag{7}$$

In which,

$$I_s=\sum_{N_{c_\Omega}}\int_{\Omega(s)}\left[U_{ik}(\xi,y_s)-\frac{\nu}{(1-\nu)\lambda^2}U_{i\alpha,\alpha}(\xi,y_S)\delta_{3k}\right]F_k(y_s)\mathrm{d}\Omega_s(y_s) \tag{8}$$

where (N_{c_Ω}) denotes the number of the overall supporting cells. $F_k(y_s)$ denotes three unknown generalized forces for each supporting cell. The field point (y_s) denotes supporting cell center. Considering the discretized form of the problem, Eq. (7) could be re-written as follows (after

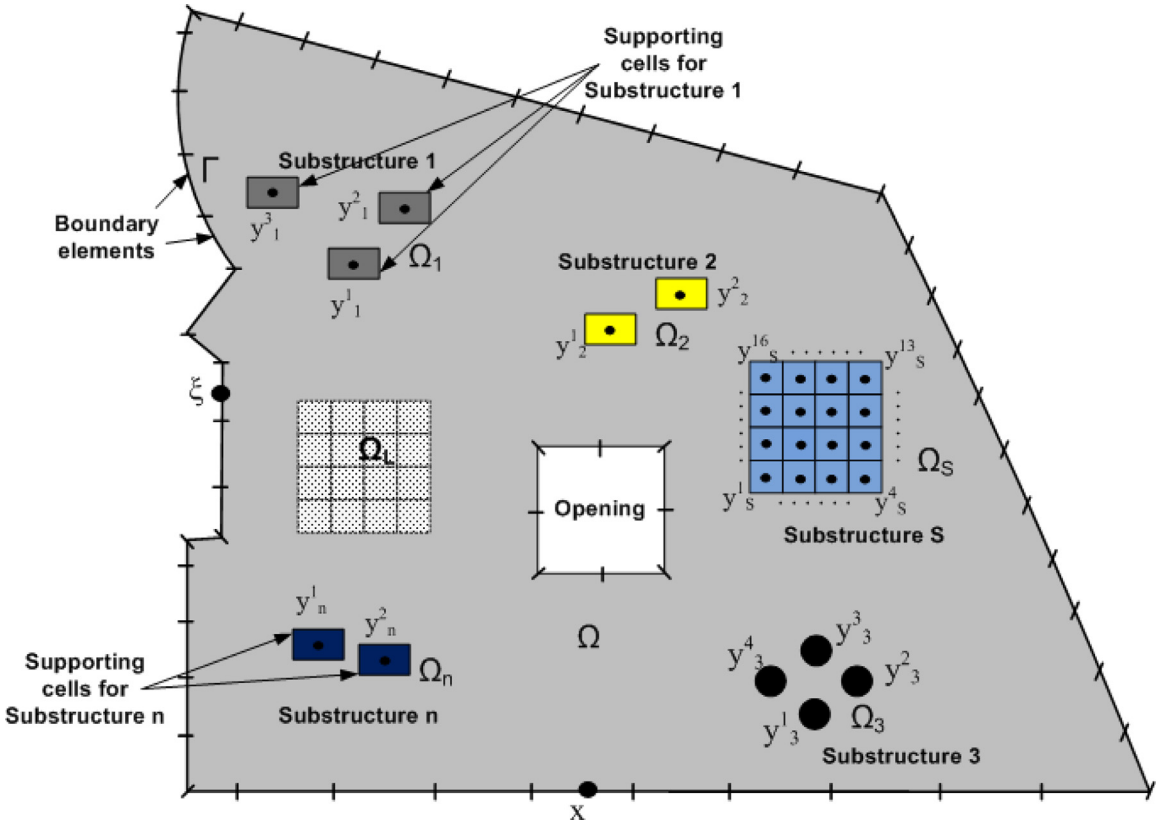

Fig. 1. General plate supported on series of substructures.

recalling the notation of Eq. (5)):

$$\begin{array}{c} \\ 3N \\ \end{array}\begin{array}{c} \begin{array}{cccccc} 3N & 3Nc_1 & 3Nc_2 & 3Nc_3 & 3Nc_s & 3Nc_n \end{array} \\ \begin{bmatrix} [A] & [B_1] & [B_2] & [B_3] & [B_s] & [B_n] \end{bmatrix} \end{array} \times \begin{array}{c} \begin{array}{c} 1 \end{array} \\ \begin{bmatrix} \{u\} \text{ or } \{t\} \\ \{F(y_1)\} \\ \{F(y_2)\} \\ \{F(y_3)\} \\ \{F(y_s)\} \\ \{F(y_n)\} \end{bmatrix} \end{array} = \begin{array}{c} \begin{array}{c} 1 \end{array} \\ \begin{bmatrix} \{LV\} - \{PBV\} \end{bmatrix} \end{array} \quad (9)$$

where $[B_s]$ are influences matrices corresponding to the following integral at cell point (y_s):

$$[B_s] = \sum_{m=1}^{N_{c_{\Omega s}}} \int_{\Omega(s)} \left[U_{ik}(\xi, y_s) - \frac{\nu}{(1-\nu)\lambda^2} U_{i\alpha,\alpha}(\xi, y_S)\delta_{3k} \right] F_k(y_s) \mathrm{d}\Omega_s(y_s) \quad (10)$$

in which $N_{c_{\Omega s}}$ denotes the number of the supporting cells in substructure (S). The vector $\{F(y_s)\}$ contains the unknown values corresponding to generalized forces at supporting cells. It has to be noted that Eq. (9) contains three additional unknowns at each supporting cell. In order to match the number of equations to the number of unknowns, another collocation scheme should be carried out at each supporting cell center to generate three extra equations, as follows:

$$u_i(Y_s^m) + \int_{\Gamma(x)} T_{ij}(Y_s^m, x) u_j(x) \mathrm{d}\Gamma(x) = \int_{\Gamma(x)} U_{ij}(Y_s^m, x) t_j(x) \mathrm{d}\Gamma(x) + L_3 + L_4 + I_d \quad (11)$$

In which,

$$L_3 = \int_{\Gamma(x)} \left[V_{i,n}(Y_s^m, x) - \frac{\nu}{(1-\nu)\lambda^2} U_{i\alpha}(Y_s^m, x) n_\alpha(x) \right] q(x) \mathrm{d}\Gamma(x) \quad (12)$$

$$L_4 = \sum_{N_{cell}} \int_{\Omega(L)} \left[U_{ik}(Y_s^m, L) - \frac{\nu}{(1-\nu)\lambda^2} U_{i\alpha,\alpha}(Y_s^m, L)\delta_{3k} \right] P_k(L) \mathrm{d}\Omega(L) \quad (13)$$

$$I_d = \sum_{p=1}^{p=n} \sum_{a=1}^{a=N_{c_{\Omega s}}} \int_{\Omega(p)} \left[U_{ik}\left(Y_s^m, y_p^a\right) - \frac{\nu}{(1-\nu)\lambda^2} U_{i\alpha,\alpha}\left(Y_s^m, y_p^a\right)\delta_{3k} \right] \times F_k\left(y_p^a\right) \mathrm{d}\Omega\left(y_p^a\right) \quad (14)$$

where Y_s^m is a new source point located at each supporting cell center (m) in substructure (S). L_3, L_4, I_d are similar integrals to L_1, L_2, I_s except when the source point is replaced by Y_s^m. Eq. (11) could be re-written

in a matrix form as follows:

	3N	$3Nc_1$	$3Nc_2$	$3Nc_3$	$3Nc_s$	$3Nc_n$	$3Nc_1$	$3Nc_2$	$3Nc_3$	$3Nc_s$	$3Nc_n$			1			1
$3Nc_1$	$[C_1]$	$[D_{11}]$	$[D_{12}]$	$[D_{13}]$	$[D_{1s}]$	$[D_{1n}]$	[I]	[0]	[0]	[0]	[0]		3N	{u} or {t}	=	$3Nc_1$	$\{LV_1\}$ - $\{PBV_1\}$
$3Nc_2$	$[C_2]$	$[D_{21}]$	$[D_{22}]$	$[D_{23}]$	$[D_{2s}]$	$[D_{2n}]$	[0]	[I]	[0]	[0]	[0]		$3Nc_1$	$\{F(y_1)\}$		$3Nc_2$	$\{LV_2\}$ - $\{PBV_2\}$
$3Nc_3$	$[C_3]$	$[D_{31}]$	$[D_{32}]$	$[D_{33}]$	$[D_{3s}]$	$[D_{3n}]$	[0]	[0]	[I]	[0]	[0]	×	$3Nc_2$	$\{F(y_2)\}$		$3Nc_3$	$\{LV_3\}$ - $\{PBV_3\}$
$3Nc_s$	$[C_s]$	$[D_{s1}]$	$[D_{s2}]$	$[D_{s3}]$	$[D_{ss}]$	$[D_{sn}]$	[0]	[0]	[0]	[I]	[0]		$3Nc_3$	$\{F(y_3)\}$		$3Nc_s$	$\{LV_s\}$ - $\{PBV_s\}$
$3Nc_n$	$[C_n]$	$[D_{n1}]$	$[D_{n2}]$	$[D_{n3}]$	$[D_{ns}]$	$[D_{nn}]$	[0]	[0]	[0]	[0]	[I]		$3Nc_s$	$\{F(y_s)\}$		$3Nc_n$	$\{LV_n\}$ - $\{PBV_n\}$
													$3Nc_n$	$\{F(y_n)\}$			
													$3Nc_1$	$\{u(y_1)\}$			
													$3Nc_2$	$\{u(y_2)\}$			
													$3Nc_3$	$\{u(y_3)\}$			
													$3Nc_s$	$\{u(y_s)\}$			
													$3Nc_n$	$\{u(y_n)\}$			

(15)

where $[C_s]$ are influences matrices corresponding to unknown generalized displacements or tractions at the boundary point (x) when the collocation point is taken as (Y_s^m). $[D]$ are influences matrices corresponding to integrals in the form I_d. The vector $\{u(y_s)\}$ contains the unknown values of generalized displacements at supporting cells. The vector $\{LV_s\}$ contains domain loading and loading cells $(L_3 + L_4)$ effects due to the second collocation scheme in Eq. (11). The vector $\{PBV_s\}$ contains prescribed boundary integral values due to the second collocation scheme in Eq. (11).

Using Eqs. (9) and (15), the matrix form of the overall problem could be re-written as follows:

		$3Nc_1$	$3Nc_2$	$3Nc_3$	$3Nc_s$	$3Nc_n$	$3Nc_1$	$3Nc_2$	$3Nc_3$	$3Nc_s$	$3Nc_n$						
$3Nc_1$	$[C_1]$	$[D_{11}]$	$[D_{12}]$	$[D_{13}]$	$[D_{1s}]$	$[D_{1n}]$	[I]	[0]	[0]	[0]	[0]		$3Nc_1$	$\{F(y_1)\}$		$3Nc_1$	$\{LV_1\}$ - $\{PBV_1\}$
$3Nc_2$	$[C_2]$	$[D_{21}]$	$[D_{22}]$	$[D_{23}]$	$[D_{2s}]$	$[D_{2n}]$	[0]	[I]	[0]	[0]	[0]		$3Nc_2$	$\{F(y_2)\}$		$3Nc_2$	$\{LV_2\}$ - $\{PBV_2\}$
$3Nc_3$	$[C_3]$	$[D_{31}]$	$[D_{32}]$	$[D_{33}]$	$[D_{3s}]$	$[D_{3n}]$	[0]	[0]	[I]	[0]	[0]		$3Nc_3$	$\{F(y_3)\}$		$3Nc_3$	$\{LV_3\}$ - $\{PBV_3\}$
$3Nc_s$	$[C_s]$	$[D_{s1}]$	$[D_{s2}]$	$[D_{s3}]$	$[D_{ss}]$	$[D_{sn}]$	[0]	[0]	[0]	[I]	[0]		$3Nc_s$	$\{F(y_s)\}$		$3Nc_s$	$\{LV_s\}$ - $\{PBV_s\}$
$3Nc_n$	$[C_n]$	$[D_{n1}]$	$[D_{n2}]$	$[D_{n3}]$	$[D_{ns}]$	$[D_{nn}]$	[0]	[0]	[0]	[0]	[I]		$3Nc_n$	$\{F(y_n)\}$		$3Nc_n$	$\{LV_n\}$ - $\{PBV_n\}$
													$3Nc_1$	$\{u(y_1)\}$			
													$3Nc_2$	$\{u(y_2)\}$			
													$3Nc_3$	$\{u(y_3)\}$			
													$3Nc_s$	$\{u(y_s)\}$			
													$3Nc_n$	$\{u(y_n)\}$			

(16)

The stiffness relationship between the generalized displacements at supporting cells $\{u(y_s)\}$ and forces $\{F(y_s)\}$ could be written as follows:

$$[K(y_s)] \times \{u(y_s)\} = \{F(y_s)\} \tag{17}$$

where: $K(y_s)$ is the stiffness matrix of supporting cells. Using Eq. (17), Eq. (16) could be re-written as follows:

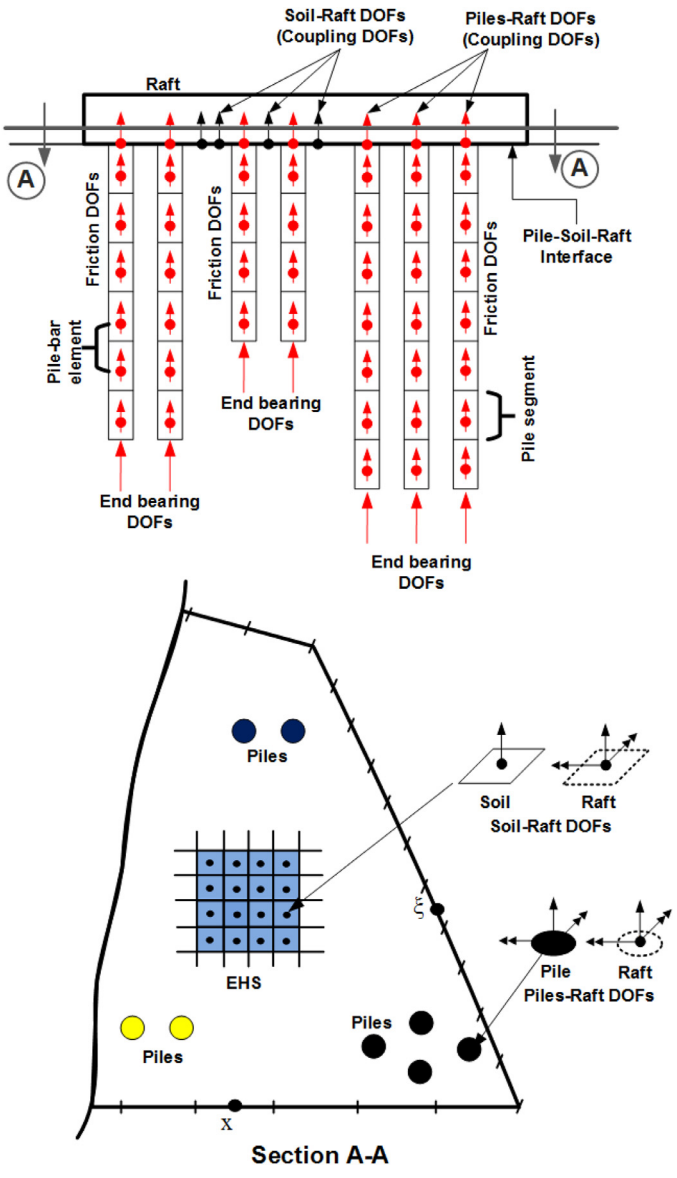

Fig. 2. General postulated pile–soil–raft degrees of freedom.

	3N	$3Nc_1$	$3Nc_2$	$3Nc_3$	$3Nc_s$	$3Nc_n$			1			1
3N	[A]	$[B_1]\times[K(y_1)]$	$[B_2]\times[K(y_2)]$	$[B_3\times[K(y_3)]$	$[B_s]\times[K(y_s)]$	$[B_n]\times[K(y_n)]$		3N	{u} or {t}	=	3N	{LV} - {PBV}
$3Nc_1$	$[C_1]$	$[D_{11}]\times[K(y_1)]$ +[I]	$[D_{12}]\times[K(y_2)]$	$[D_{13}]\times[K(y_3)]$	$[D_{1s}]\times[K(y_s)]$	$[D_{1n}]\times[K(y_n)]$		$3Nc_1$	$\{u(y_1)\}$		$3Nc_1$	$\{LV_1\}$ - $\{PBV_1\}$
$3Nc_2$	$[C_2]$	$[D_{21}]\times[K(y_1)]$	$[D_{22}]\times[K(y_2)]$ +[I]	$[D_{23}]\times[K(y_3)]$	$[D_{2s}]\times[K(y_s)]$	$[D_{2n}]\times[K(y_n)]$	×	$3Nc_2$	$\{u(y_2)\}$		$3Nc_2$	$\{LV_2\}$ - $\{PBV_2\}$
$3Nc_3$	$[C_3]$	$[D_{31}]\times[K(y_1)]$	$[D_{32}]\times[K(y_2)]$	$[D_{33}]\times[K(y_3)]$ +[I]	$[D_{3s}]\times[K(y_s)]$	$[D_{3n}]\times[K(y_n)]$		$3Nc_3$	$\{u(y_3)\}$		$3Nc_3$	$\{LV_3\}$ - $\{PBV_3\}$
$3Nc_s$	$[C_s]$	$[D_{s1}]\times[K(y_1)]$	$[D_{s2}]\times[K(y_2)]$	$[D_{s3}]\times[K(y_3)]$	$[D_{ss}]\times[K(y_s)]$ +[I]	$[D_{sn}]\times[K(y_n)]$		$3Nc_s$	$\{u(y_s)\}$		$3Nc_s$	$\{LV_s\}$ - $\{PBV_s\}$
$3Nc_n$	$[C_n]$	$[D_{n1}]\times[K(y_1)]$	$[D_{n2}]\times[K(y_2)]$	$[D_{n3}]\times[K(y_3)]$	$[D_{ns}]\times[K(y_s)]$	$[D_{nn}]\times[K(y_n)]$ +[I]		$3Nc_n$	$\{u(y_n)\}$		$3Nc_n$	$\{LV_n\}$ - $\{PBV_n\}$

(18)

Eq. (18) represents a general matrix formulation to analyze a plate supported over a number of substructures knowing the stiffness matrix of each supporting structure.

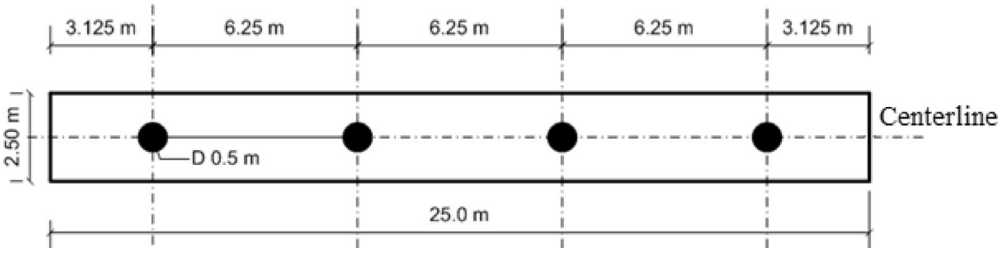

Fig. 3. Pile cap geometry presented in example 6.1.

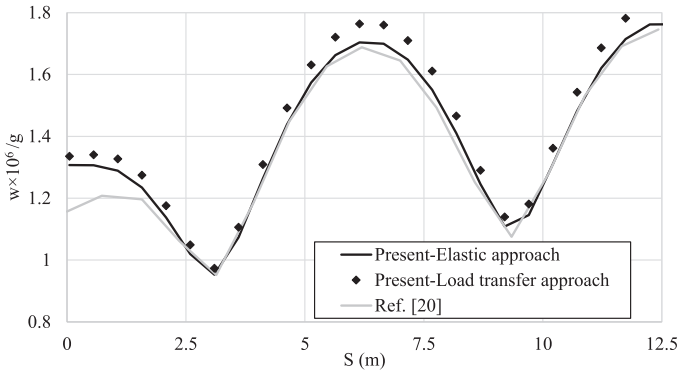

Fig. 4. Deflection along centerline strip for case $t = 0.079$ m.

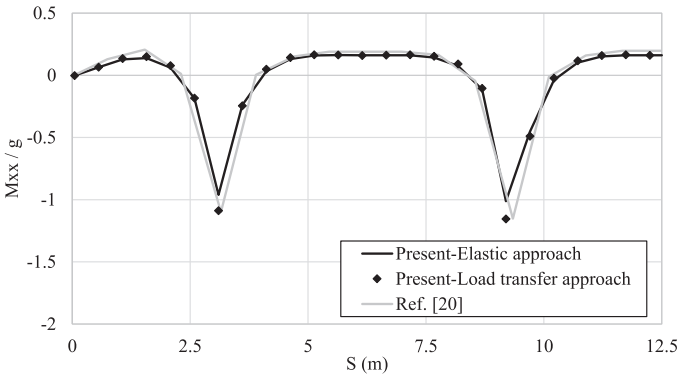

Fig. 5. Bending moments along centerline strip for case $t = 0.079$ m.

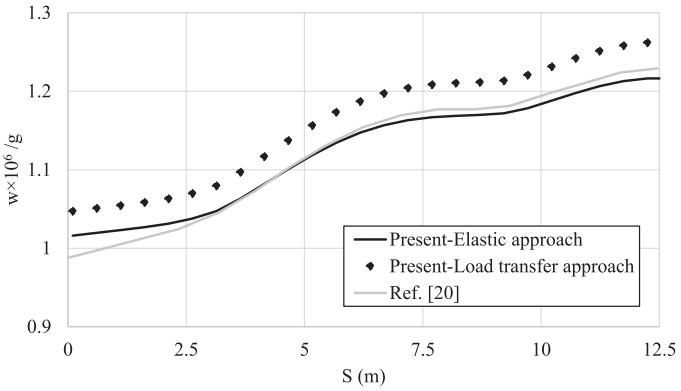

Fig. 6. Deflection along centerline strip for case $t = 0.37$ m.

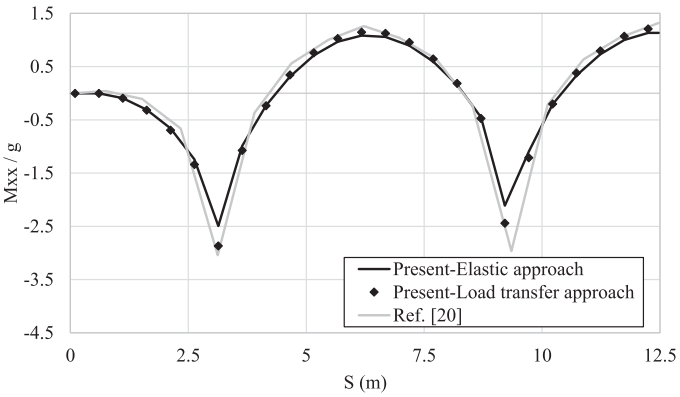

Fig. 7. Bending moments along centerline strip for case $t = 0.37$ m.

4. Piled raft interactions

A general piled raft consists of raft supported on a soil–pile system. In this paper, a raft is modeled as a thick plate in bending. The soil is considered as elastic half space (EHS) and discretized into a series of internal supporting cells under the raft domain; each has one degree of freedom (DOF) as shown in Fig. 2. Although the raft plate has three DOF, the interaction between raft and soil (EHS) is considered only along the direction of the settlement DOF. Piles are considered as internal (w.r.t. the raft plate) supporting circular cells [33] and are modeled through the soil as bar elements. Each pile is divided into a number of divisions; each division has one axial degree of freedom to simulate the friction effects between pile and soil medium (friction DOF). The pile element is considered as the link between two DOFs. It has to be noted that friction is assumed constant along each pile segment. Additionally two degrees of freedom are postulated. One at the top point connecting the raft to the pile (coupling DOF) and the other at the bottom tip (End bearing DOF) of the pile as demonstrated in Fig. 2.

In this section, the overall flexibility matrix ([F] as shown in Eq. (19)) of soil–pile system is computed. This includes all interaction effects.

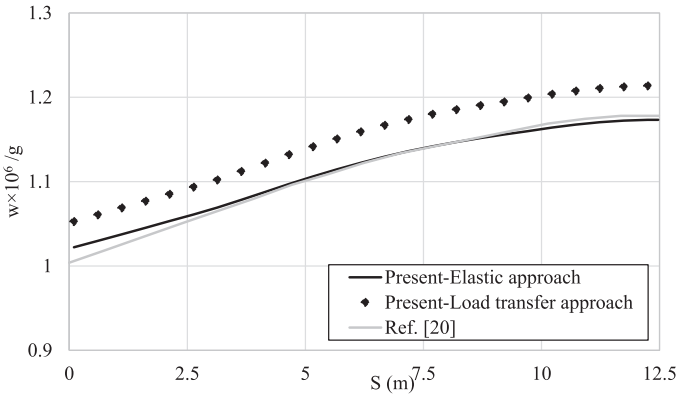

Fig. 8. Deflection along centerline strip for case $t = 0.79$ m.

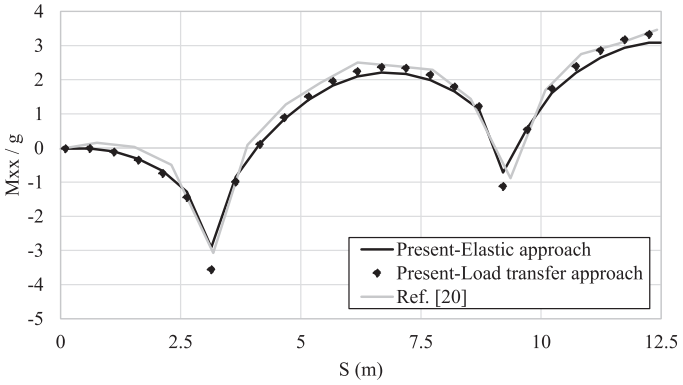

Fig. 9. Bending moments along centerline strip for case $t = 0.79$ m.

Three main flexibility cases are considered: Soil–soil, Soil–pile or Pile–soil, and Pile–pile (recall Eq. (19)):

$$[F] = \begin{array}{c|cc} & \text{Soil DOFs} & \text{Piles DOFs} \\ \hline \text{Soil DOFs} & \text{S-S} & \text{S-P} \\ \text{Piles DOFs} & \text{P-S} & \text{P-P} \end{array} \tag{19}$$

(1) The soil–soil (S–S) case: the flexibility coefficients are computed when load is applied at a certain soil DOF and displacement is computed at any other soil DOF. Herein, the computation are based on Mindlin's [29], or Boussinesq's [30], or Steinbrenner's [31] solutions as previously presented by Shaaban and Rashed [16]. It has to be noted that Mindlin's solution for point load involves singular values. Therefore, the closed form solution presented in [16] is used for rectangular soil cells.

(2) Pile–soil (P–S) or Soil–pile (S–P) case: the flexibility coefficients are computed between a certain soil DOF and a pile DOF (friction, end bearing, or coupling DOF). It could be considered based on Mindlin's solution; in which the settlement at pile node is computed due to unit load applied at a soil degree of freedom or vice versa.

(3) Pile–pile (P–P) case: the flexibility coefficients are computed by two different methods: the elastic approach [1] (based on Mindlin's equation), or the load transfer approach (based on Randolph empirical formulas [2]). Pile–pile flexibility coefficients could also be partitioned into three parts: friction part, end bearing part, and coupling part as given in Eq. (20).

$$[F] = \begin{array}{c|cccc} & \text{Soil DOFs} & \text{Friction DOFs} & \text{End bearing DOFs} & \text{Coupling DOFs} \\ \hline \text{Soil DOFs} & \text{S-S} & \text{S-P}_f & \text{S-P}_e & \text{S-P}_c \\ \text{Friction DOFs} & \text{P}_f\text{-S} & \text{P}_f\text{-P}_f & \text{P}_f\text{-P}_e & \text{P}_f\text{-P}_c \\ \text{End bearing DOFs} & \text{P}_e\text{-S} & \text{P}_e\text{-P}_f & \text{P}_e\text{-P}_e & \text{P}_e\text{-P}_c \\ \text{Coupling DOFs} & \text{P}_c\text{-S} & \text{P}_c\text{-P}_f & \text{P}_c\text{-P}_e & \text{P}_c\text{-P}_c \end{array} \tag{20}$$

All off-diagonal terms of pile–pile interaction effects (such as P_f–P_e, P_f–P_c, P_e–P_c) are computed based on Mindlin's solution [29]. It has to be noted that in case of computing the diagonal values of P_f–P_f, P_e–P_e, P_c–P_c, Mindlin's solution for point load presents singular values; therefore, two closed form solutions are derived to treat these singular values. The first is for friction DOFs (P_f–P_f); in such a case, flexibility coefficients (f_{ij}) are calculated using cylindrical shaft element via the following integral (See Appendix A):

$$f_{ij} = \frac{1}{2\Pi r_o \ell} \int_0^{2\pi} \int_{\ell_1}^{\ell_2} f_{ij} r_o \mathrm{d}\ell \, \mathrm{d}\theta \tag{21}$$

where r_o, ℓ, ℓ_1, and ℓ_2 are pile radius, pile element length, depth of the start point of loaded element, and depth of the end point of loaded element, respectively. The second is the case of end bearing (P_e–P_e) or

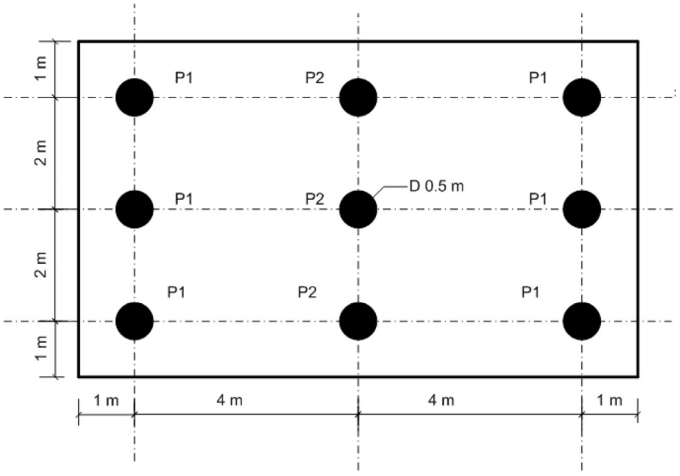

Fig. 10. Piled raft geometry presented in example 6.2.

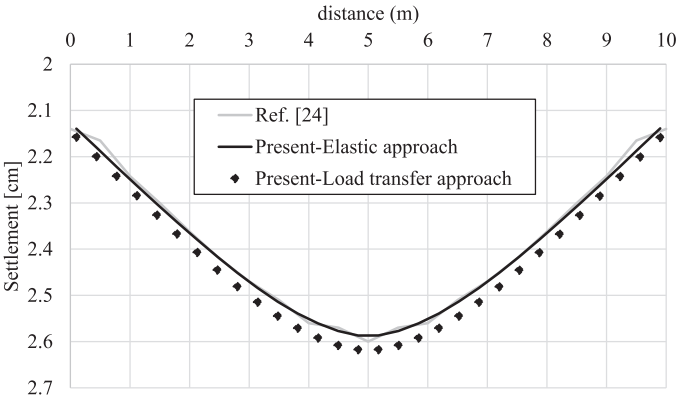

Fig. 11. Settlement along centerline strip.

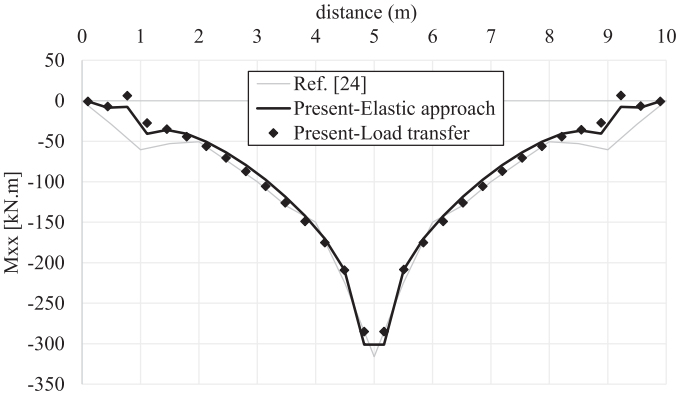

Fig. 12. Bending moments along centerline strip.

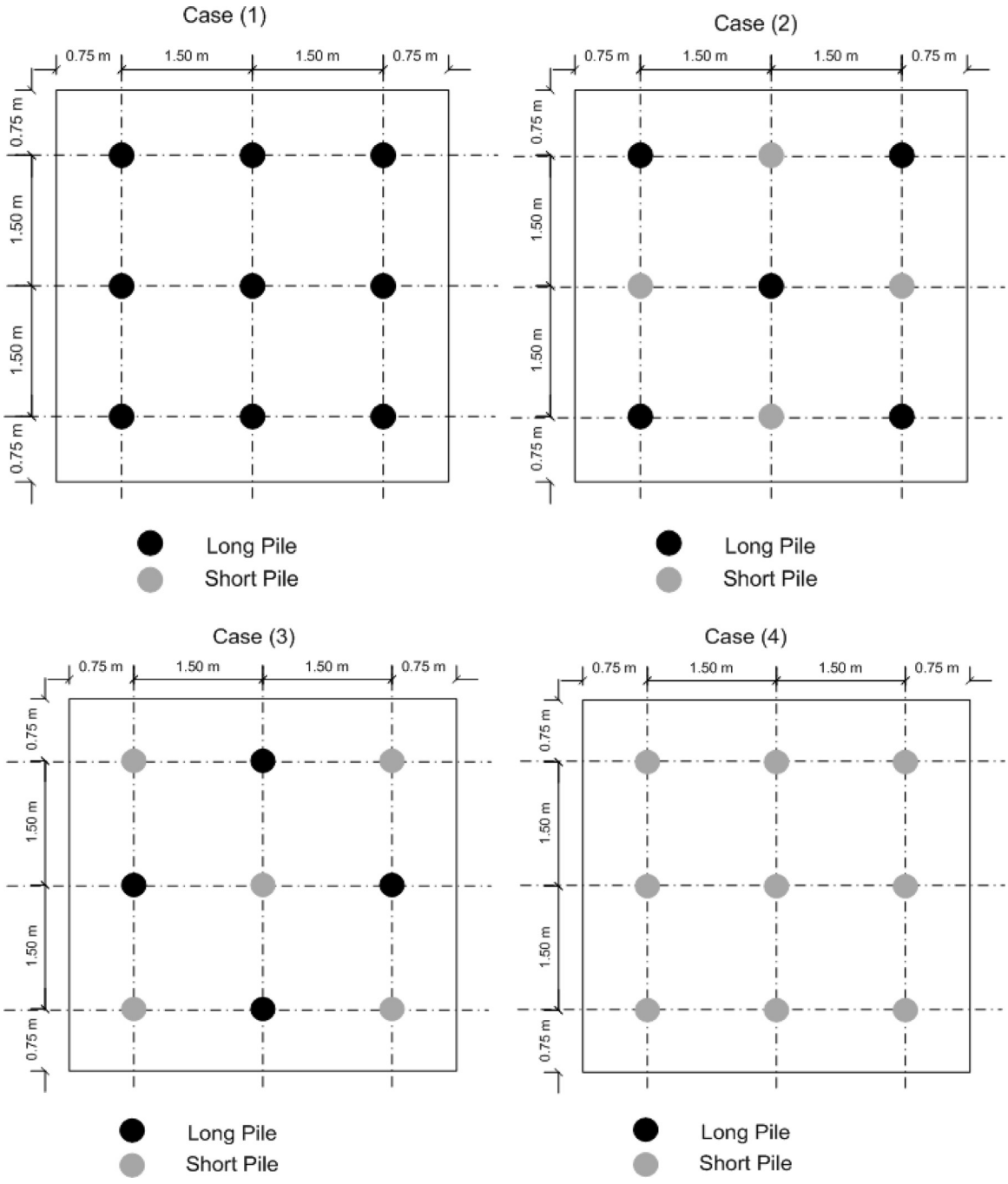

Fig. 13. Four cases of piles configurations and raft geometry.

the case of coupling DOFs (P_c–P_c). In such cases, flexibility coefficients are calculated using a circular element via the following integral (See Appendix B):

$$f_{ij} = \frac{1}{\Pi {r_o}^2} \int_0^{2\pi} \int_0^{r_0} f_{ij} r \mathrm{d}r \mathrm{d}\theta \tag{22}$$

5. The soil–pile system as added stiffness

Interaction effects presented in the previous section are used to generate the overall flexibility matrix Eq. (20) of the soil–pile system. The overall stiffness matrix of a soil–pile system is calculated as the inverse of this flexibility matrix. Then, axial deformation stiffness matrix of pile elements is added to the overall stiffness matrix of soil–pile system. In order to avoid generating huge systems of coupled equations, all degrees of freedom away from the pile–soil–raft interface are eliminated using the well-known static condensation process. The overall soil–pile system stiffness matrix size is decreased from $[\mathrm{K}]_{\mathrm{NDOF}\times\mathrm{NDOF}}$ to $[K]_{N_{cells}\times N_{cells}}$, where NDOF is defined in Eq. (23) and N_{cells} is the total number of soil and pile cells at pile–soil–raft interface (coupling DOFs, recall Fig. 2).

$$\mathrm{NDOF} = \left(\sum_{N_{\mathrm{piles}}} N_{\mathrm{pile\ divisions}} \right) + 2 + N_{\mathrm{soil\ cells}} \tag{23}$$

Hence, the obtained condensed soil–pile stiffness matrix including all interaction effects is considered as the supporting substructure to be added to the integral equation as presented in Section 3. It has to be

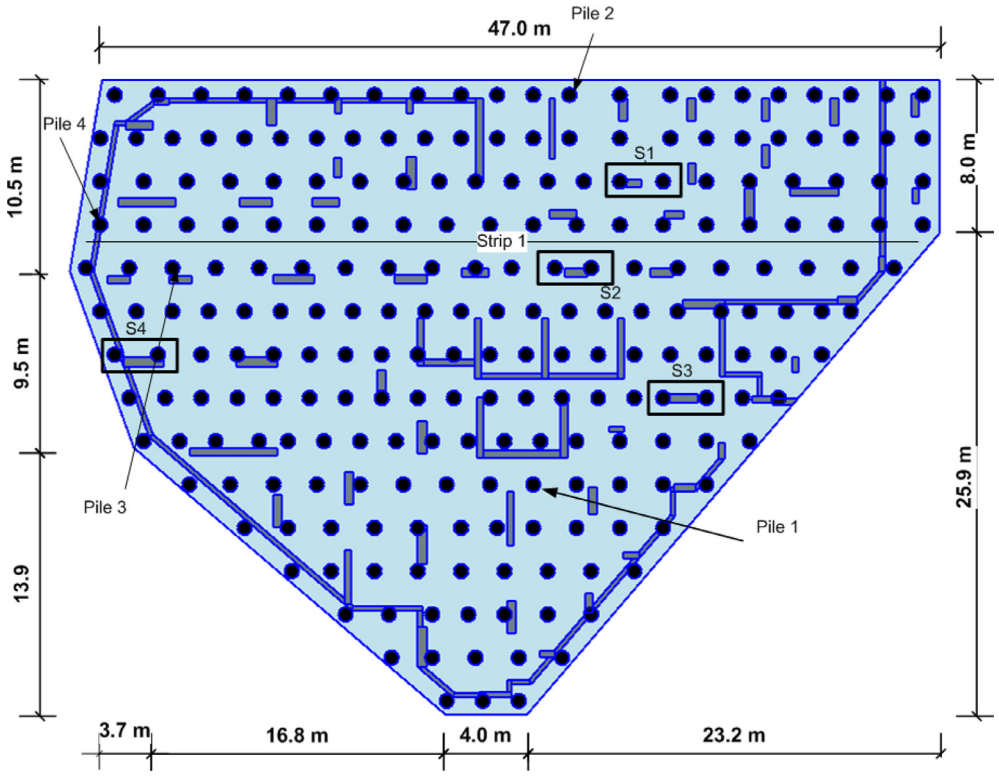

Fig. 14. Practical example geometry.

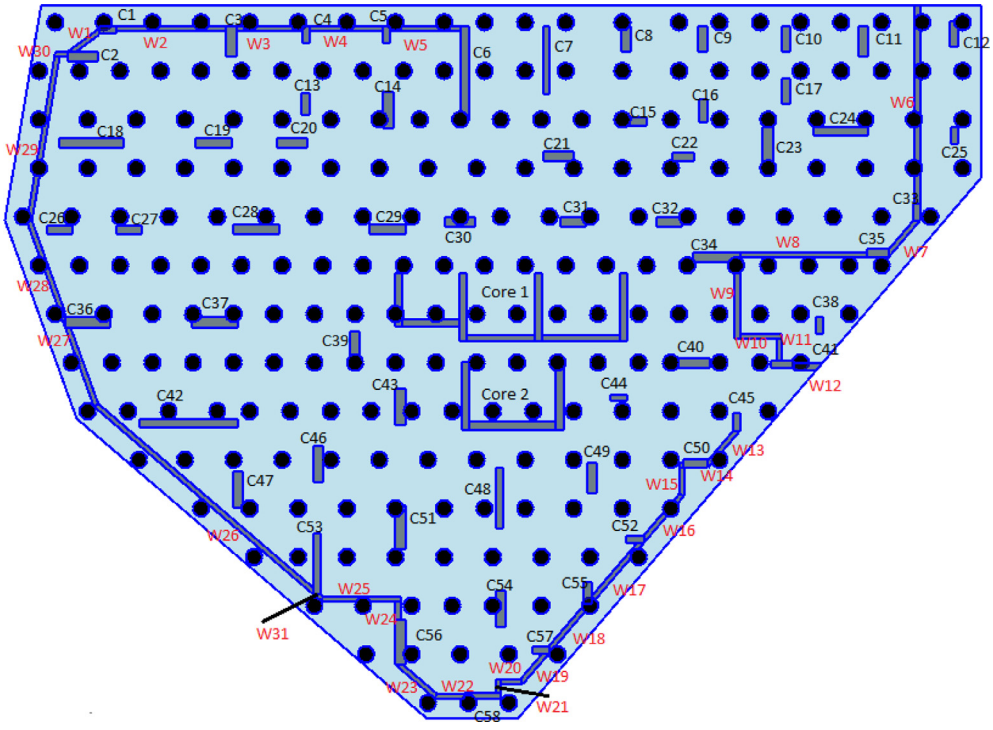

Fig. 15. Columns and wall loads ID.

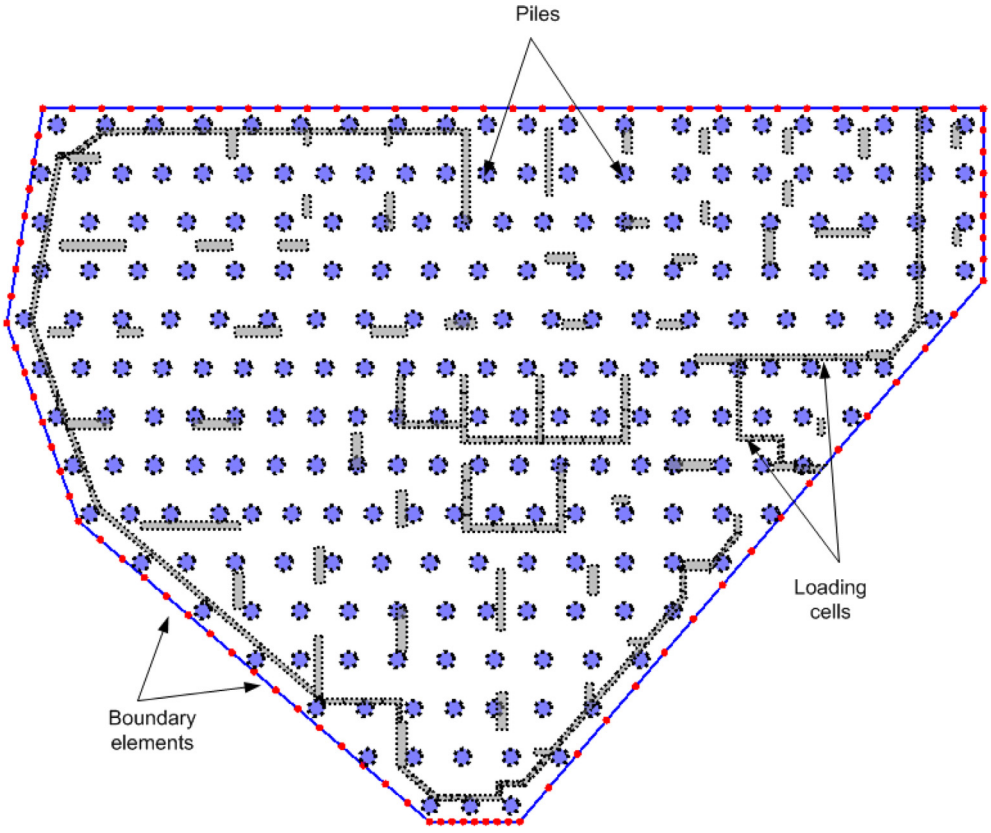

Fig. 16. BEM model of practical example.

Table 1
Number of DOFs before and after condensation process.

	Before condensation process	After condensation process
No. of DOFs	183	79

Table 2
Number of DOFs before and after condensation process.

	Before condensation process	After condensation process
No. of DOFs	168	69

noted that other substructures stiffness matrices could be also added to the presented formulation beyond soil–pile system as substructure such as beams, drops, or any other supporting structures (e.g., diaphragm walls, etc.).

6. Numerical examples and applications

In this section, several examples are presented and results are compared to previously published results. A practical example is then presented to demonstrate the strength of using the proposed boundary element formulation in the analysis of practical engineering applications.

6.1. Pile cap supported on four piles (compared to Ref. [20])

The pile cap supported on four piles and shown in Fig. 3 is considered. The pile diameter is 0.5 m; length is 25 m. Soil modulus of elasticity is 2000 kN/m^2, and Poisson's ratio is 0.5. The pile cap is loaded by uniform load (g) and is modeled with three different thicknesses (0.079, 0.37, 0.79 m) to allow comparison to results of Ref. [20]. The soil is divided into 25×3 rectangular elements. Piles are divided into 50 cylindrical elements and two circular elements for end bearing and coupling DOFs. In [20], the boundary element method is used to model the pile cap as thin plate on elastic foundations and soil under raft is divided into triangular elements. Results are presented along the centerline strip of pile cap. Figs. 4–9 present deflection (w) and bending moments (M_{xx}) for the three cap thicknesses. Table 1 presents the number of solved DOFs before and after the condensation process. It can be seen from Figs. 4–9 that results are in good agreement with results of Ref. [20].

6.2. Raft on nine piles under circular loads (compared to Ref. [24])

The piled raft on nine piles shown in Fig. 10 is considered in this example. Piles are 10 m in length and 0.5 m in diameter. The raft is 0.5 m in thickness and subjected to circular loads $P_1 = 500$ kN and $P_2 = 1000$ kN directly on piles as shown in Fig. 10. The used modulus of elasticity for the raft and piles is 2×10^7 kN/m^2; whereas soil modulus

Table 3
Maximum settlement value (m) for different piles pattern.

	Load = 100 MPA		Load = 200 MPA		Load = 300 MPA	
	Ref. [17]	Present elastic approach	Ref. [17]	Present elastic approach	Ref. [17]	Present elastic approach
Case 1	0.0195	0.0201	0.0392	0.0402	0.0587	0.0603
Case 2	0.0213	0.0222	0.0427	0.0444	0.0643	0.0666
Case 3	0.0223	0.0225	0.0446	0.0451	0.0668	0.0676
Case 4	0.0446	0.0464	0.0883	0.0923	0.1327	0.1392

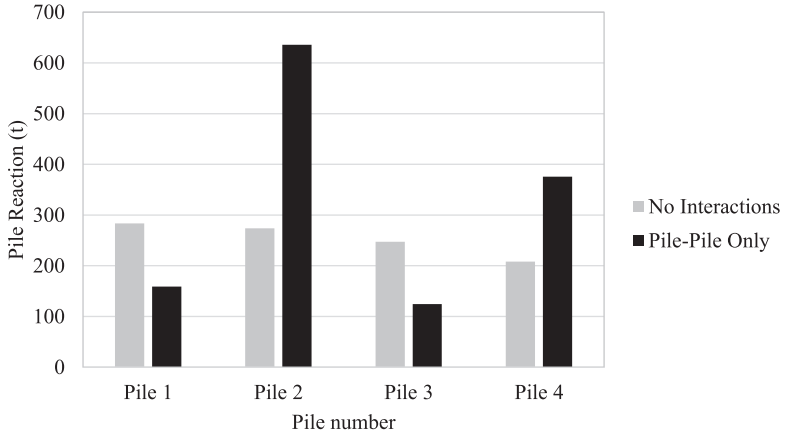

Fig. 17. Sample pile forces.

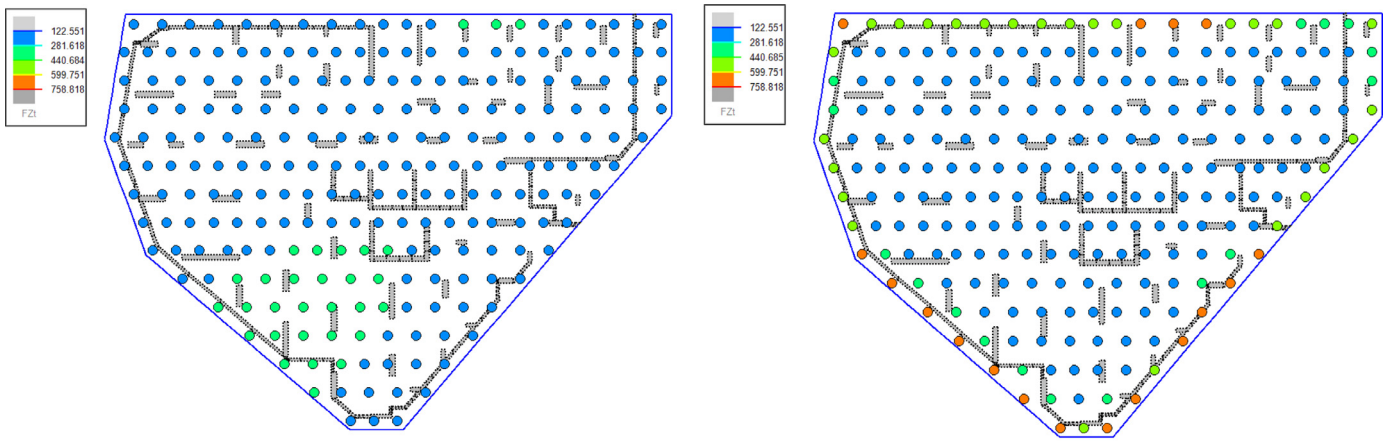

a: Without considering interaction effects. b: With considering interaction effects.

Fig. 18. Pile forces distribution. (a) Without considering interaction effects. (b) With considering interaction effects.

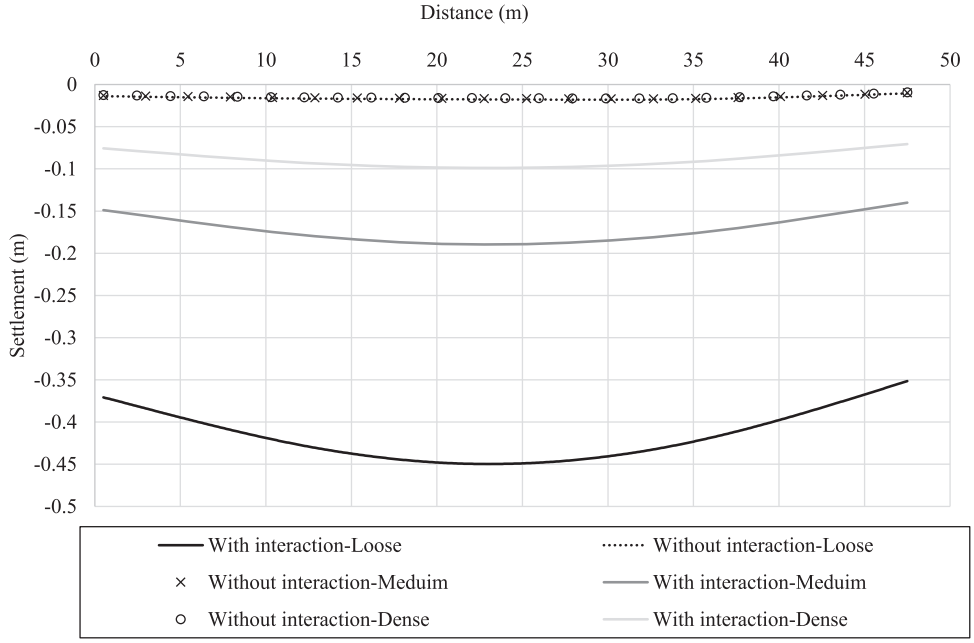

Fig. 19. Deflection values along the horizontal strip 1.

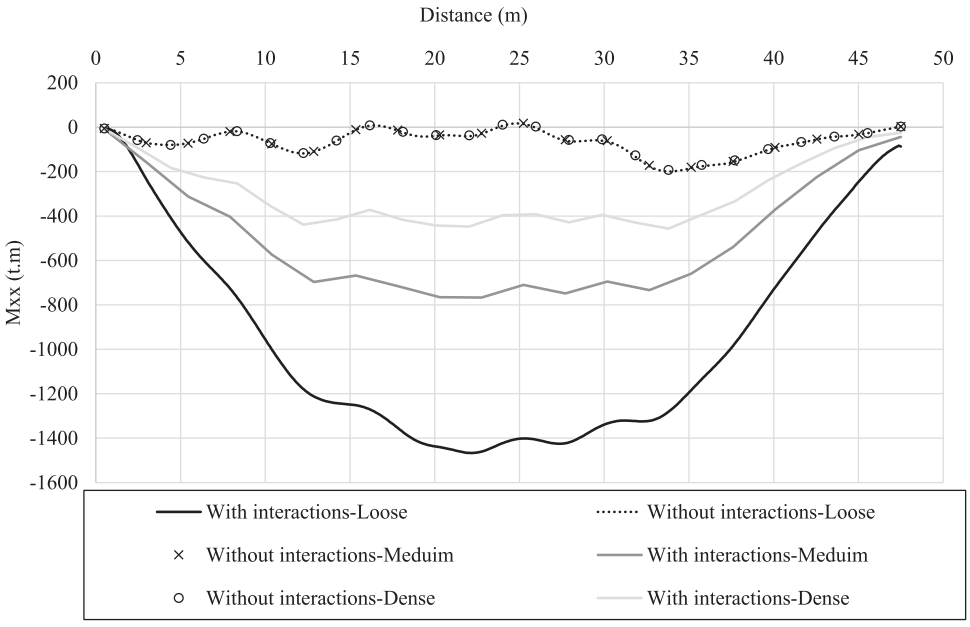

Fig. 20. Bending moment values along the horizontal strip 1.

Table 4
Number of DOFs before and after condensation process.

Case	DOFs before condensation process	DOFs after condensation process
1	324	90
2	244	90
3	224	90
4	144	90

of elasticity is 20,000 kN/m^2 and Poisson's ratio is 0.3. The raft is modeled as thick plate on elastic foundations and soil is divided into 10×6 rectangular elements and each pile is divided into 10 cylindrical elements and two circular element for end bearing and coupling DOFs. In Ref. [24], the finite element method is used to model the raft as thin plate on elastic foundations using the ELPLA software [24]. In [24], the raft is divided into 10×6 elements and each pile is divided into10 elements. Results are presented along centerline strip of the raft. Figs. 11 and 12 demonstrate settlement and bending moments along centerline strip, respectively. It has been seen that proposed technique results are in good agreement with the FEM results in [24]. Table 2 presents the number of DOFs before and after condensation process.

6.3. Piled raft with variable lengths of piles (compared to Ref. [17])

A piled raft supported on nine piles and subjected to uniform load q_v (kN/m^2) is considered in this example. The purpose of this example is to compare the presented formulation results to results of Ref. [17] for piles with different lengths, which are based on modeling the soil as 3D finite elements. Piles, are 0.5 m in diameter and classified as long and short piles with lengths 25, 5 m, respectively. The raft dimensions is $4.5\times4.5\times1.0$ m. Modulus of elasticity of raft, long piles, and short piles are 3.0×10^7, 2.0×10^7, and 1.7×10^7 kN/m^2, respectively. Soil modulus of elasticity is 5000 kN/m^2 and Poisson's ratio is 0.35. The raft is modeled as thick plate on elastic foundations and soil is divided into 9×9 rectangular elements. Each pile is divided using 1 m cylindrical element and two circular element for end bearing and coupling DOFs. It has to be noted that, the load transfer approach is not applicable for this case; therefore, this example is solved using the elastic approach only.

Table 5
Columns, walls and cores loads.

Column ID	Load (t)	Column ID	Load (t)	Wall ID	Load (t/m')
C1	247.8	C31	603.42	W1	1.67
C2	655.5	C32	603.42	W2	5.43
C3	745.02	C33	200.36	W3	3.27
C4	152.34	C34	1335.76	W4	3.69
C5	218.42	C35	410.54	W5	3.49
C6	1602.58	C36	1298.73	W6	9.75
C7	1085.1	C37	1335.24	W7	2.11
C8	637.08	C38	445.36	W8	6.24
C9	653.58	C39	938.4	W9	3.79
C10	583.2	C40	1268.32	W10	2.08
C11	835.2	C41	421.96	W11	1.05
C12	612.72	C42	2119.88	W12	1.778
C13	476.24	C43	938.4	W13	2.16
C14	1013.22	C44	324.48	W14	0.183
C15	664.12	C45	249.6	W15	1.34
C16	502.4	C46	1063.98	W16	2.87
C17	614.56	C47	1008.9	W17	3.7
C18	1168.2	C48	1265.6	W18	2.97
C19	1038.9	C49	780.06	W19	1.84
C20	847.38	C50	590.04	W20	1.04
C21	723.78	C51	1271.2	W21	0.67
C22	509.44	C52	326.93	W22	1.39
C23	998.52	C53	1340.1	W23	2.33
C24	1130.32	C54	996.06	W24	0.93
C25	236.64	C55	501.65	W25	3.86
C26	592.2	C56	1155.3	W26	14.11
C27	663.6	C57	248.08	W27	4.07
C28	1386.64	C58	555.56	W28	5.2
C29	1020.16	Core 1	3293.68	W29	8.23
C30	873.06	Core 2	184.32	W30	0.63
				W31	0.34

In [17], the finite element method is used to model raft as thick plate on 3D finite elements using the ANSYS software. In this example, the four cases of pile configurations (see Fig. 13) are solved. Table 3 presents the maximum settlement of the raft under three different uniform loads 100, 200, and 300 MPa. It has be seen that results are in a good agreement to those in Ref. [17]. Table 4 demonstrates the number of DOFs before and after condensation process.

Table 6
Number of DOFs before and after condensation process.

	Before condensation process	After condensation process
No. of DOFs	8547	231

6.4. Piled raft example

The previous examples demonstrated the validity of used formulation by comparing its results to previously published results. It has to be noted that most of the previously published results consider simple rafts and pile caps. In this example, the practical piled raft foundation shown in Fig. 14 is analyzed. The raft thickness is 2.50 m and rested on 231 piles with 0.8 diameter and 35 m length. Soil modulus of elasticity is 2000 t/m^2 and Poisson's ratio is 0.3. Piles and raft modulus of elasticity is 2,210,000 t/m^2. The raft is subjected to columns and wall loads from superstructure with total vertical load of 58,714.9 t as illustrated in Table 5 and Fig. 15. Fig. 16 demonstrates the used boundary element model. The raft is modeled as thick plate on elastic foundations, each pile is divided using 1 m cylindrical element and two circular element for end bearing and coupling DOFs.

Table 7
Shearing force distribution over considered four regions.

Region	Considering interactions	Legend	Ignoring interactions
S_1	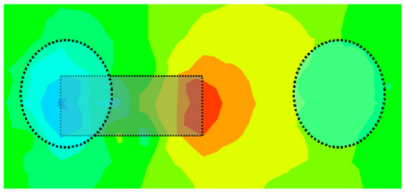	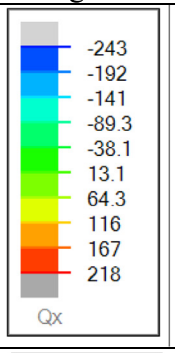	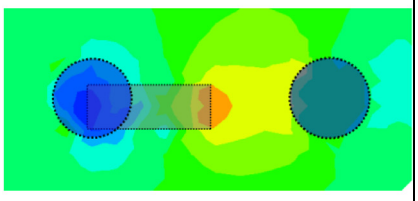
S_2	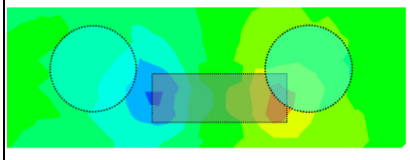	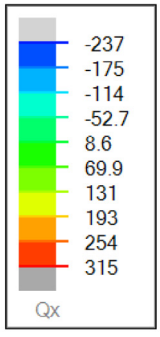	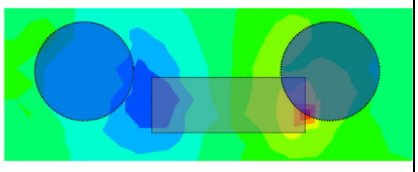
S_3	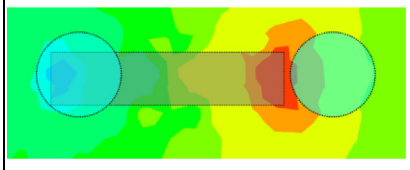	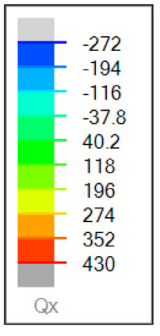	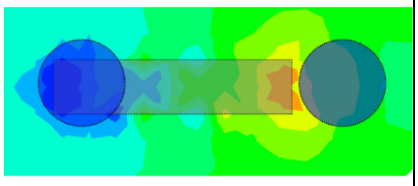
S_4	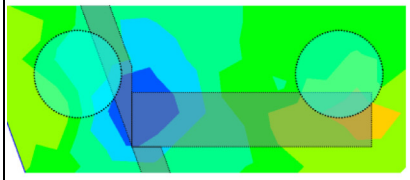	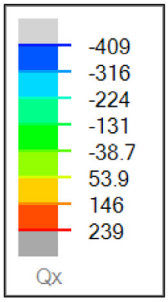	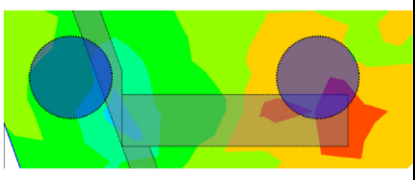

The following example is solved twice, without and with considering the interaction effects. Three different soil types [loose ($E = 2000\ t/m^2$), medium ($E = 5000\ t/m^2$), and dense ($E = 10{,}000\ t/m^2$)] are used for the sake of comparison. It has be noted that, in case of ignoring interaction effects, pile stiffness is calculated based on empirical equations used in building design code [22] to be 151,000 t/m.

Four piles are selected as demonstration sample (see Fig. 14). Piles 1 and 3 represent interior piles, whereas piles 2 and 4 represent exterior piles. Fig. 17 demonstrates the selected piles reactions considering and ignoring the interaction effects.

Fig. 18 demonstrates pile force distribution considering and ignoring the interaction effects. It can be seen that considering the interaction effects redistributes pile forces by increasing pile reaction at exterior piles rather than those at interior piles. Therefore including interaction effects is important in the design of practical examples.

Figs. 19 and 20 demonstrate the deflection and bending moment values for different soil types (loose, medium, and dense) on a horizontal strip presented in Fig. 14. It can be seen that considering interaction effects increases the predicted raft settlement. This is noticeable for loose soil. Table 6 demonstrates the advantages of the proposed condensation process to solve practical piled rafts, as DOFs decreased by about 97%.

In order to demonstrate the strength of using the BEM together with the thick plate formulation, simple punching analysis is considered in this example. Regions S_1, S_2,S_3, and S_4 are considered to draw the shear stress distribution Q_x as contour maps in Table 7 for the case of loose soil. From the presented results, it can be seen that punching shear will be critical for external piles and internal loading zones (S_3 and S_4) in case of considering interactions effects. This is opposite to the case of ignoring interaction effects, which indicates that internal piles and external loading zones are the critical ones. This confirms the importance of considering interaction effects in design of practical examples.

7. Conclusions

The analysis of practical piled rafts is presented based on boundary element formulation of thick plate and pile–soil system is added by innovative technique. All interaction types are considered, pile–pile, pile–soil, and soil–soil interactions. Pile–pile interaction is considered based on "Elastic Approach" or "Load Transfer Approach". Pile–soil interaction is considered based on Mindlin's solution. Soil–soil interaction is considered as elastic half space. Piles are divided into cylindrical elements representing friction and circular elements representing end bearing action. Piles DOFs are condensed at the pile–soil interface representing the contact between pile–soil system.

Several examples are presented and results are verified. It can be concluded that:

(1) The presented formulation is suitable for practical applications.
(2) The presented formulation models accurately pile rafts with real dimensions of applied column/wall loadings and piles; even it can compute accurately the distribution of shearing forces in vicinity of stress concentration.
(3) The used condensation technique allows analyzing huge applications with great savings.
(4) It is essential to consider the interaction effects in practical applications.

Therefore, practical engineers are encouraged to make use of the advantages of using boundary elements in real life engineering applications.

Acknowledgments

This project was supported financially by the Science and Technology Development Fund (STDF), Egypt, Grant no. 14910. The second and third authors would like to acknowledge the support of (STDF).

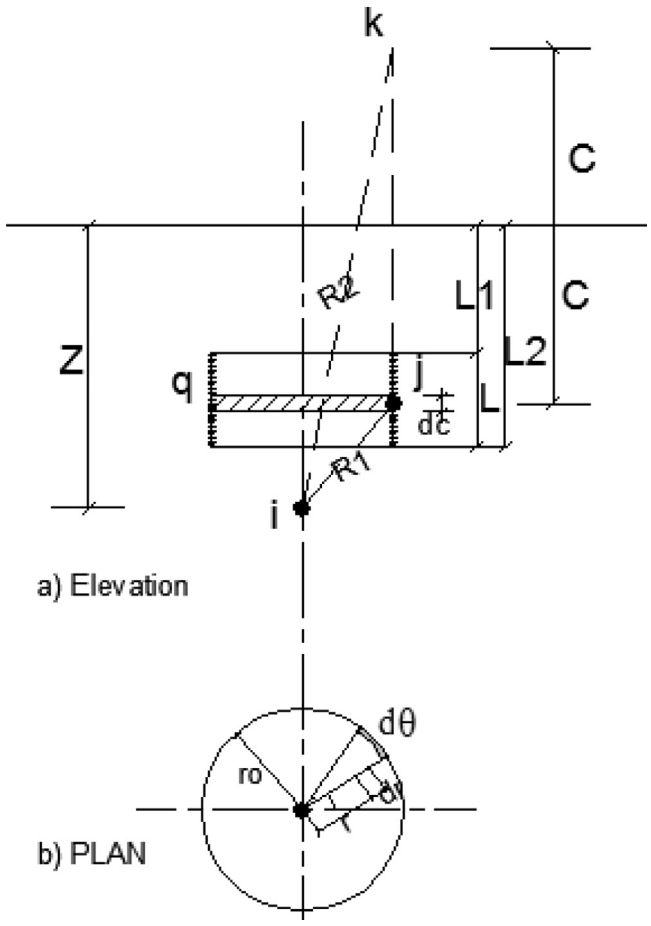

Fig. A1. Cylindrical element definitions.

Appendix A

The flexibility coefficients F_{ij} in Eq. (21) could be computed as follows, if a cylindrical element (j) is loaded (as shown in Fig. A1); the response (settlement) at element (i) could be computed as:

$$F_{ij} = \frac{1}{16\pi\ell\, G_s(1-\upsilon_s)}\left[I_1 + I_2 + I_3 + I_4 + I_5\right] \tag{A1}$$

Where:

$$I_1 = (3-4\upsilon_s)\ln\left[\frac{\sqrt{r_0^2+(Z-\ell_2)^2}-(Z-\ell_2)}{\sqrt{r_0^2+(Z-\ell_1)^2}-(Z-\ell_1)}\right] \tag{A2}$$

$$I_2 = \left(8(1-\upsilon_s)^2-(3-4\upsilon_s)\right)\ln\left[\frac{\sqrt{r_0^2+(Z+\ell_2)^2}+(Z+\ell_2)}{\sqrt{r_0^2+(Z+\ell_1)^2}+(Z+\ell_1)}\right] \tag{A3}$$

$$I_3 = \ln\left[\frac{\sqrt{r_0^2+(Z-\ell_2)^2}-(Z-\ell_2)}{\sqrt{r_0^2+(Z-\ell_1)^2}-(Z-\ell_1)}\right] + \frac{(Z-\ell_2)}{\sqrt{r_0^2+(Z-\ell_2)^2}} - \frac{(Z-\ell_1)}{\sqrt{r_0^2+(Z-\ell_1)^2}} \tag{A4}$$

$$I_4 = (3-4\upsilon_s)\left[\ln\left[\frac{\sqrt{r_0^2+(Z+\ell_2)^2}+(Z+\ell_2)}{\sqrt{r_0^2+(Z+\ell_1)^2}+(Z+\ell_1)}\right]\right.$$

$$-\frac{(Z+\ell_2)}{\sqrt{r_0^2+(Z+\ell_2)^2}}+\frac{(Z+\ell_1)}{\sqrt{r_0^2+(Z+\ell_1)^2}}\Bigg]$$
$$-2Z\Bigg[\frac{1}{\sqrt{r_0^2+(Z+\ell_1)^2}}-\frac{1}{\sqrt{r_0^2+(Z+\ell_2)^2}}$$
$$+\frac{Z(Z+\ell_1)}{r_0^2\sqrt{r_0^2+(Z+\ell_1)^2}}-\frac{Z(Z+\ell_2)}{r_0^2\sqrt{r_0^2+(Z+\ell_2)^2}}\Bigg] \quad \text{(A5)}$$

$$I_5=\frac{-2Z^2}{r_0^2}\Bigg[\frac{(Z+\ell_2)^3}{\left(r_0^2+(Z+\ell_2)^2\right)^{1.5}}-\frac{(Z+\ell_1)^3}{\left(r_0^2+(Z+\ell_1)^2\right)^{1.5}}\Bigg]$$
$$-4Z\Bigg[\frac{r_0^2+1.5(Z+\ell_2)^2}{\left(r_0^2+(Z+\ell_2)^2\right)^{1.5}}-\frac{r_0^2+1.5(Z+\ell_1)^2}{\left(r_0^2+(Z+\ell_1)^2\right)^{1.5}}\Bigg] \quad \text{(A6)}$$

where:

ℓ: pile element length.
r_0: pile radius.
G_s: soil shear modulus of pile element.
υ_s: soil Poisson's ratio of pile element
Z: depth of element node i.
C: depth of applied unit load at element node j.

Appendix B

The flexibility coefficients F_{ib} in Eq. (22) could be computed as follows, if a base circular element (b) is loaded (as shown in Fig. B1); the response (settlement) at element (i) could be computed as:

$$F_{ib}=\frac{1}{8\,\pi\, r_0^2 G_s(1-\upsilon_s)}\Bigg[(3-4\upsilon_s)\Big[-\|Z-C\|+\sqrt{r_0^2+(C-Z)^2}\Big]$$
$$+\Big(8(1-\upsilon_s)^2-(3-4\upsilon_s)\Big)\Big(\sqrt{r_0^2+(C+Z)^2}-(C+Z)\Big)$$
$$+\|Z-C\|-\frac{(Z-C)^2}{\sqrt{r_0^2+(Z-C)^2}}+\big((3-4\upsilon_s)\big((C+Z)^2\big)-2CZ\big)$$
$$\times\left(\frac{1}{C+Z}-\frac{1}{\sqrt{r_0^2+(C+Z)^2}}\right)+\frac{2CZ}{C+Z}-\frac{2CZ(C+Z)^2}{\left(r_0^2+(Z+C)^2\right)^{1.5}}\Bigg] \quad \text{(B1)}$$

Where:

Z: depth of element node i.
C: depth of applied unit load at base node b.

In case of calculate the response at base due to load on the same base, Z will be equal C therefore; Eq. (B1) will be as follows:

$$F_{bb}=\frac{1}{8\,\pi\, {r_0}^2 G_s(1-\upsilon_s)}\Big[(3-4\upsilon_s)[r_o]+\Big(8(1-\upsilon_s)^2-(3-4\upsilon_s)\Big)$$
$$\times\Big(\sqrt{{r_0}^2+4Z^2}-2Z\Big)+\big((3-4\upsilon_s)(2Z^2)\Big(\frac{1}{2Z}-\frac{1}{\sqrt{{r_0}^2+4Z^2}}\Big)$$
$$+Z-\frac{8Z^4}{({r_0}^2+4\,Z^2)^{1.5}}\Big] \quad \text{(B2)}$$

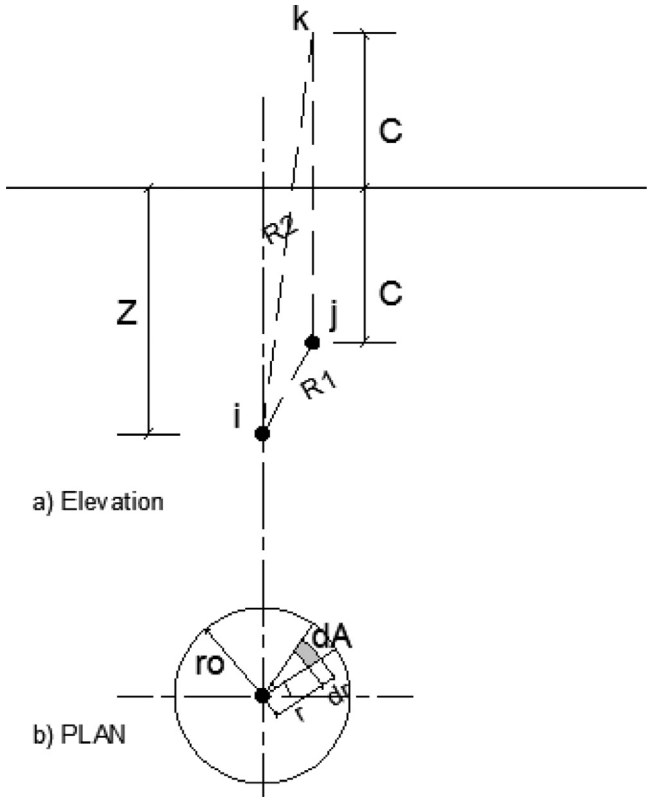

Fig. B1. Circular element definitions.

In case of calculate the response at pile head (top point) due to load on the same point, Z will be equal C and equal to zero therefore; Eq. (B1) will be as follows:

$$F_{tt}=\frac{1}{8\,\pi\, {r_0}^2 G_s(1-\upsilon_s)}\Big[(3-4\upsilon_s)[r_o]+\Big(8(1-\upsilon_s)^2-(3-4\upsilon_s)\Big)(r_o)\Big] \quad \text{(B3)}$$

Where:

Z, C: depth of the pile top node (t) = zero.

References

[1] Poulos HG, Davis EH. The settlement behavior of single axially loaded incompressible piles and piers. Geotechnique 1968;18:351–71.
[2] Randolph MF, Worth CP. Analysis of deformation of vertically loaded piles. J Geotech Eng Div ASCE 1978;104:1465–88.
[3] Poulos HG, Davis EH. Pile foundation analysis and design. New York, NY: John Wiley and Sons; 1980.
[4] Poulos HG. A Report Prepared on Behalf of Technical CommitteeTC18 on Piled Foundations. International Society of Soil Mechanics and Geotechnical Engineering 2001.
[5] Coduto DP. Foundation design – principles and practices. The United States of America: Pearson – Prentice Hall; 2001.
[6] Cheung YK, Zienkiewicz OC. Plates and tanks on elastic foundations-an application of finite element method. Int J Solids Struct 1965;1:451–61.
[7] Svec OJ, McNEICE GM. Finite element analysis of finite sized plates bonded to an elastic half space. Comput Methods Appl Mech Eng 1972;1:265–77.
[8] Svec OJ, Gladwel GM. A triangular plate bending element for contact problems. Int J Solids Struct 1973;9:435–46.
[9] Rajapakse RK, Selvadurai AP. The performance of Mindlin plate elements in modeling plate-elastic medium interaction: a comparative study. Int J Numer Methods Eng 1986;23:1229–44.
[10] Katsikadelis JT, Armenakas AE. Plates on elastic foundation by BIE method. J Eng Mech 1984;110:1086–105.
[11] Syngellakis S, Bai SC. The application of the boundary element method to plate-half space interaction. Eng Anal Bound Elem 1993;12:119–25.
[12] de Paiva JB, Butterfield R. Boundary element analysis of plate-soil interaction. Comput Struct 1997;64:319–28.
[13] Rashed YF, Aliabadi MH, Brebbia CA. The boundary element method for thick plates on a Winkler foundation. Int J Numer Methods Eng 1998;41:1435–62.
[14] Rashed YF, Aliabadi MH. Boundary element analysis of buildings foundation plates. Eng Anal Bound Elem 2000;24:201–6.

[15] Rashed YF. A boundary/domain element method for analysis of building raft foundations. Eng Anal Bound Elem 2005;29:859–77.
[16] Shaaban AM, Rashed YF. A coupled BEM-stiffness matrix approach for analysis of shear deformable plates on elastic half space. Eng Anal Bound Elem 2013;37:699–707.
[17] Moayed RZ, Izadi E, Mirsepahi M. 3D finite elements analysis of vertically loaded composite piled raft. J Cent South Univ 2013;20:1713–23.
[18] Wulandaria PR, Tjandraa T. Analysis of piled raft foundation in soft soil using PLAXIS 2D. Proc Eng 2015;125:363–7.
[19] Trondi RR, de Paiva JB. Boundary element analysis of capped and uncapped pile groups. Adv Eng Softw 1999;30:715–24.
[20] Mendonca AV, de Paiva JB. A boundary element method for the static analysis of raft foundations on piles. Eng Anal Bound Elem 2000;24:237–47.
[21] Small JC. Practical solutions to soil – structure interaction problems. Prog Struct Eng Mater 2001;3(3):305–14. doi:10.1002/pse.87.
[22] National Housing and Construction Research Center. Code of Practice for Soil Mechanics – Part 4: Deep Foundations.
[23] Dang DCN, Seong-Bae J, Dong-Soo K. Design method of piled-raft foundations under vertical load considering interaction effects. Comput Geotech 2013;47:16–27.
[24] ELPLA software, geotecsoftware.com.
[25] LUSAS software, http://www.lusas.com.
[26] PLAXIS software, www.plaxis.com.
[27] ABAQUS software, www.3ds.com/products-services/simulia/products/abaqus/.
[28] Midas software, www.midas.com.
[29] Wang CM, Chow YK, How YC. Analysis of rectangular thick rafts on an elastic half space. Compute Geotech 2001;28:161–84.
[30] Selvadurai APS. Elastic analysis of soil foundation interaction. Amsterdam: Elsevier; 1979.
[31] Bowels JE. Foundation analysis and design. 5th Ed. New York: McGraw-Hill; 1996.
[32] Vander F. Application of the boundary integral equation method to Reissner's plate model. Int J Numer Methods Eng 1982;18:1–10.
[33] Mehanny SSF, Mehanny SSF, Rashed YF. A probabilistic boundary element method applied to the pile dislocation problem. Eng Struct 2011;33:2919–30.